Chapter 1

Synthetic Design Guided by Oxidation Pattern Analysis[†]

1.1 INTRODUCTION

With complex molecular structures, intriguing oxidation patterns, and wide-ranging biological activities, natural products have greatly impacted research in organic chemistry and drug discovery. Diterpenes, in particular, have long drawn the attention of synthetic chemists due to their diverse and fascinating molecular architectures. These are coupled to a wide range of biological activities, and promising anticancer, antibacterial, and antimalarial activities have inspired multimillion-dollar campaigns to develop complex diterpenes, such as paclitaxel, pleuromutilin, and artemisinin, as therapeutics.[1]

Over the past decade, many efforts have been directed toward the synthesis of complex and highly oxygenated diterpenes using functional group-guided topological strategies.[2] These efforts highlight how the preparation of diterpenes by chemical- or

[†]Portions of this chapter were adapted from the following communication: Dibrell, S. E.; Tao, Y.; Reisman, S. E. *Acc. Chem. Res.* **2021**, *54* (6), 1360–1373.

semi-synthesis can transform our ability to use such molecules and their synthetic derivatives as biological probes or as lead compounds for the development of new medicines. Nonetheless, the elaborate polycyclic systems and intricate oxidation patterns that characterize many diterpenes can still hinder traditional medicinal chemistry studies of their biological activity.[3] New advances in the science of chemical synthesis, driven both by the invention of new reactions and strategies, are required to provide flexible and modular access to this important class of natural products.

Figure 1.1 *Synthetic strategies guided by oxidation pattern analysis*

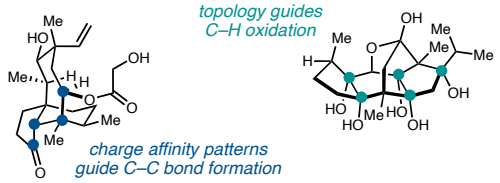

In this introductory chapter, we present completed total syntheses of several highly oxidized diterpenes and show how analysis of oxidation patterns and inherent functional group relationships can inform key C–C bond disconnections that greatly simplify the complexity of polycyclic structures and streamline their syntheses (Figure 1.1). The approaches to synthetic strategy are based on the formalism that heteroatoms impose an alternating acceptor and donor reactivity pattern upon a carbon skeleton, a particularly useful idea when considering oxidized natural products as synthetic targets. Two major themes emerge. First, reductive cyclizations are strategic umpolung tactics for building polycyclic systems with dissonant oxidation patterns. Second, unexpected, emergent reactivity can be leveraged to effectively balance early-stage oxidation with topology-guided oxidative manipulations at a late stage. We hope that collective

discussion of the selected diterpene natural products conveys how oxidation pattern analysis can guide effective synthetic design.

1.1.1 *Overview of Oxidized Diterpene Syntheses*

The syntheses discussed can be roughly grouped into two types of strategies, both of which were guided by consideration of the oxidation pattern of the target (Figure 1.2).

Figure 1.2 *Oxidized diterpene natural products*

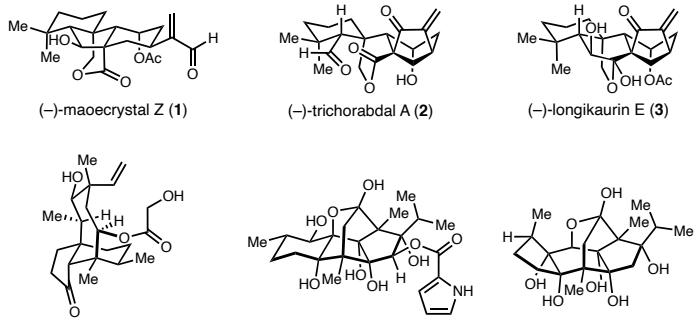

The first group includes the *Isodon* diterpenoids maoecrystal Z (**1**), trichorabdal A (**2**), and longikaurin E (**3**), and the antibiotic pleuromutilin (**4**); each possesses a key γ-hydroxyketone motif embedded within its polycyclic framework. The γ-hydroxyketone is an example of what Evans classified a 'dissonant' charge affinity pattern: the polarization imparted along the carbon chain between the oxygen functional groups is mismatched (Figure 1.3).[5b,5c] Carbon–carbon bond formation within this dissonant path requires a polarity inversion, or as Seebach defined, 'reactivity umpolung'.[5c] The position of this dissonant charge affinity pattern in each structure inspired synthetic strategies involving ring closure by Sm-mediated addition of an aldehyde-derived ketyl radical to an α,β-unsaturated cabonyl.[4,5] These syntheses highlight how this tactic is especially effective when used to simultaneously form rings and introduce 1,4-dioxygenation patterns.

Figure 1.3 *Oxidation guides C–C bond formation*

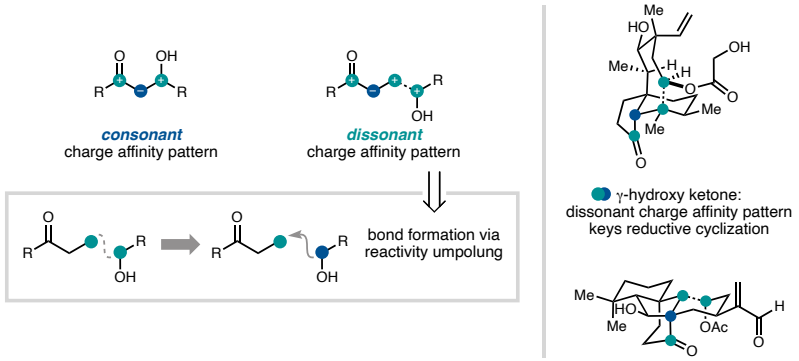

The second group includes the targets ryanodine (**5**) and perseanol (**6**), which required a different strategy to address their high degree of oxidation (Figure 1.4). In these systems, the oxidation was introduced in two stages: (1) in the first few steps of the synthesis, prior to construction of the primary carbon framework; and (2) at a late stage, through strategic deployment of C–H oxidation reactions. In both syntheses, nearly all oxidation is introduced in the required oxidation state, with the correct stereochemistry, avoiding lateral functional group manipulations.

Figure 1.4 *Topology guides oxidation*

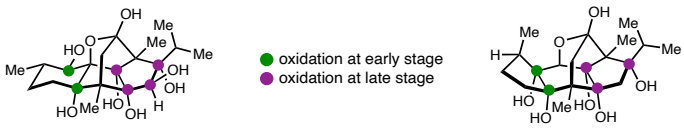

1.2 ADDRESSING DISSONANT CHARGE AFFINITY PATTERNS

1.2.1 ent-*Kauranoid Diterpenes*

Plants of the *Isodon* genus are often used in Chinese traditional medicine and are the source of over 600 *ent*-kauranoid diterpenes.[6,7] The parent compound, *ent*-kaurene, is the first cyclic diterpene produced as part of the gibberellin biosynthetic pathway in

plants and fungi.[8] One large subfamily of *ent*-kauranoids bears oxidation at C20. Examples of these natural products include (–)-longikaurin E (**3**), the 6,7-*seco*-*ent*-kauranoid (–)-trichorabdal A (**2**), and the rearranged 6,7-*seco*-*ent*-kauranoid (–)-maoecrystal Z (**1**).[11a,9] Recognizing that these *ent*-kauranoids share oxidation at C7, C11, and C20, a unified strategy was envisioned which might provide access to all three targets. In the biosynthetic pathway, *ent*-kaurene is oxidized and rearranges to **1**, **2**, and **3**; an abiotic approach could incorporate key oxidized functional groups in spiro-lactone **8**, then form the C6–C7 and C9–C11 bonds through reductive cyclizations.

Figure 1.5 *Retrosynthetic analysis of* ent-*kauranoid diterpenes*

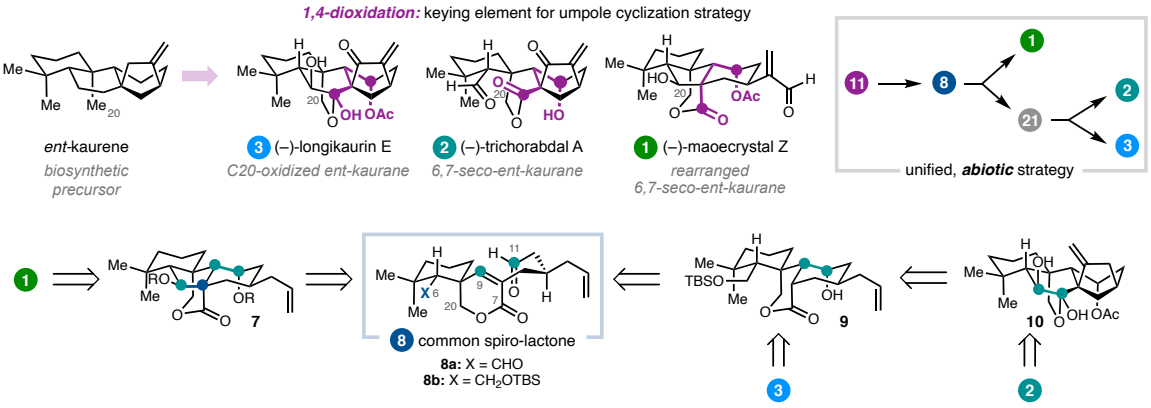

The general strategy was guided by identification of the γ-hydroxyketone motif spanning C7 to C11 (Figure 1.5).[10] This dissonant charge affinity pattern keyed the use of a SmI_2-mediated reductive cyclization to generate an umpole at the C11 position. In the context of preparing maoecrystal Z, use of a dialdehyde (**8a**) was envisioned to enable a cascade process;[8,9] initial formation of the C9–C11 bond followed by single electron reduction would give the corresponding enolate, which could undergo an intramolecular aldol reaction to close the central five-membered ring.[11] Alternatively, SmI_2-mediated monocyclization of **8b**, followed by subsequent oxidative cyclization to form the

requisite bicyclo[3.2.1]octane, could enable elaboration to trichorabdal A (**3**) and longikaurin E (**4**).

Figure 1.6 *12-Step total synthesis of (–)-maoecrystal Z*

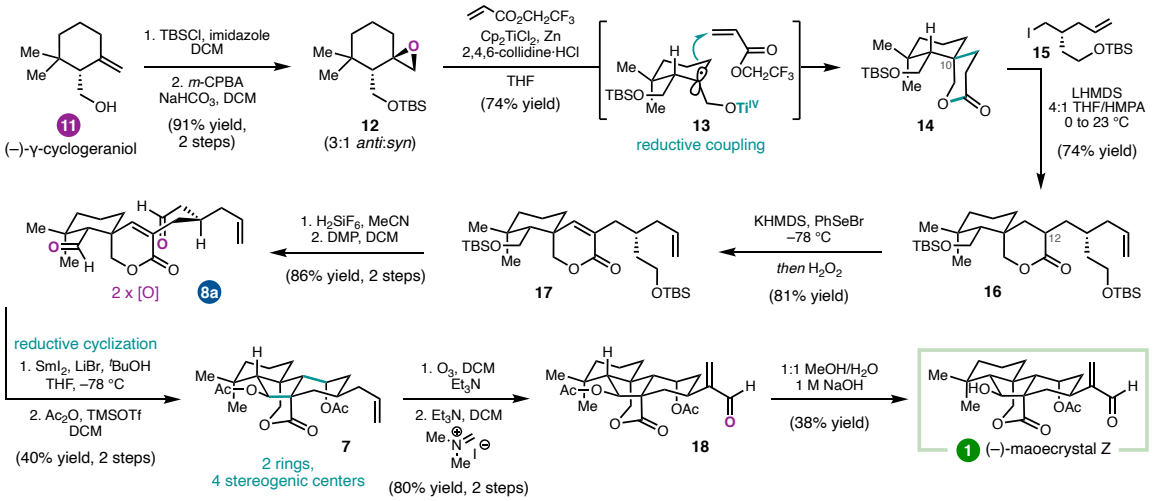

With (–)-**1** as a first target,[12] the Ti^{III}-mediated reductive coupling of **12** with a variety of acrylates initially investigated, with the goal of incorporating the requisite side chain to minimize steps after lactone formation (Figure 1.6). Whereas the use of simple acrylates, such as methyl acrylate, gave **14** as the product in varying yield, acrylates with α-substituents failed to undergo the desired coupling. Fortunately, use of 2,2,2-trifluoroethyl acrylate as an electrophilic partner under modified Gansäuer conditions[13] led to the isolation of lactone **14** as a single diastereomer in good yield. The reaction presumably proceeds through radical intermediate **13**, in which approach of the acrylate from opposite the large siloxymethylene group affords the desired C10 stereochemistry. Alkylation of the lactone followed by desaturation, desilylation, and oxidation gave dialdehyde **8a**.

In the key SmI_2-mediated reductive cyclization, lithium salts were found to be critical for desired reactivity. Treatment of dialdehyde **8a** with SmI_2 in the presence of

LiBr and ^{t}BuOH as a proton source thus provided the tetracyclic diol, which was isolated as a single diastereomer. This transformation builds two rings and introduces two secondary carbinols in a single step. In fact, the cascade reaction was critical to forming the central five-membered ring; attempts to form the two rings sequentially, in a non-cascade process, failed to identify conditions that engage the C6 aldehyde derived from tricycle **9** (see Fig. 1.7) in the intramolecular aldol. Diacetylation, ozonolysis, and methenylation gave enal **18**, which upon mono-deacetylation delivered (–)-maoecrystal Z (**1**) in 12 linear steps from (–)-γ-cyclogeraniol (**11**).[1]

Figure 1.7 *Total synthesis of (–)-longikaurin E and (–)-trichorabdal A*

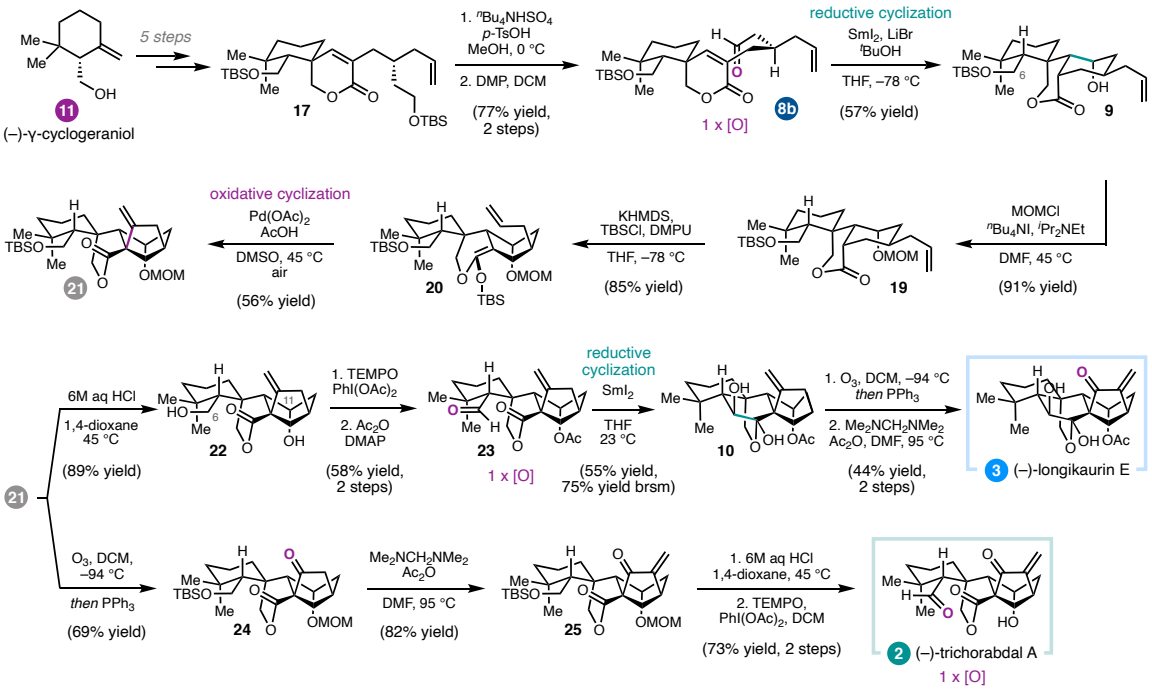

In order to access trichorabdal A and longikaurin E,[14] the key spiro-lactone was utilized, and selective deprotection/oxidation of **17** was executed to prepare **8b** (Figure 1.7). Fortunately, subjection of monoaldehyde **8b** to the previously developed reductive cyclization conditions gave tricycle **9** as a single diastereomer, which was protected as

the methoxymethyl ether. Taking inspiration from Pd-catalyzed oxidative cyclizations of silyl enol ethers,[15] a similar aerobic transformation of a silyl ketene acetal was envisioned that could establish the final carbocyclic ring and leverage the pendant alkene without need for further functionalization. Indeed, following extensive reaction development, subjection of **20** to stoichiometric $Pd(OAc)_2$ in DMSO provided tetracycle **21**.

At this stage, intermediate **21** was diverted to targets (–)-**3** and (–)-**2** through slightly different reaction sequences. Global deprotection of **21** followed by selective oxidation at C6 and acetylation at C11 provided aldehyde **23**. A SmI_2-mediated intramolecular aldehyde–lactone pinacol coupling afforded lactol **10** as a single diastereomer, another example of the strategic use of SmI_2 to introduce dissonant oxidation patterns via C–C bond formation. Finally, ozonolysis and methenylation gave (–)-**3** in 17 steps (longest linear sequence) from **11**. Alternatively, **21** could be advanced to **25** through ozonolyis and methenylation. Acidic deprotection and oxidation then revealed the aldehyde of (–)-**2**.[17]

The unified strategy enabled the first total syntheses of three architecturally distinct *ent*-kauranoids from a common intermediate and illustrates the utility of single-electron reduction chemistry for the preparation of congested polycyclic systems bearing dissonant oxidation patterns.

1.2.2 *Pleuromutilin*

The fungal diterpene (+)-pleuromutilin (**4**), first isolated in 1951, inhibits bacterial protein synthesis,[16] and semi-synthetic analogues have been advanced into the clinic as antibiotics.[17] Importantly, amine-containing 12-*epi*-**4** derivatives have been reported as

efficacious against gram-negative pathogens.[18] With the goal of providing enabling chemistry for the synthesis of new mutilin-based antibacterial agents, a concise and flexible syntheses of both **4** and its C12 epimer was sought.[19] Three prior syntheses[20] of **4** all built the eight-membered ring relatively early in the synthesis, requiring lengthy sequences to then introduce the C10-C11-C12 stereotriad. In this synthetic planning, building the eight-membered ring by annulation with a functionalized C10–C14 fragment was envisioned in order to minimize functional group manipulations after tricyclic core formation (Figure 1.8).

Figure 1.8 *Retrosynthetic analysis of (+)-pleuromutilin*

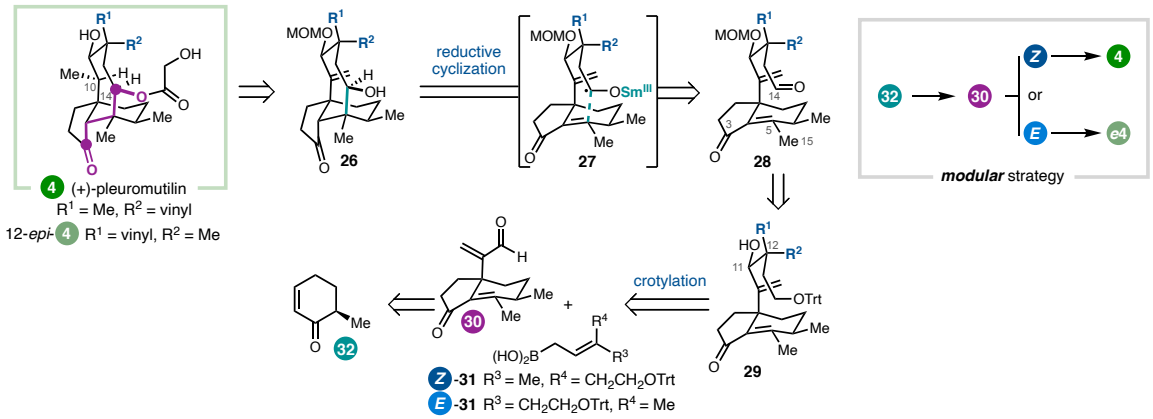

Similar to the approach to the *Isodon ent*-kauranoids, the dissonant γ-hydroxyketone pattern from C3 to C14 was identified as a keying element for a SmI_2-mediated reductive cyclization to form the C5–C14 bond. Although Procter had previously employed a SmI_2-mediated cascade cyclization for the synthesis of **4**,[22c,d] the design of that cascade required an ester at C15 to induce a ketyl radical conjugate addition. As a result, the Procter approach required several additional steps to adjust the oxidation states at C3 and C15. In contrast, a SmI_2-mediated cyclization of **28** was expected to provide **26** with C3, C14, and C15 in the correct oxidation states.

Having identified this reductive cyclization tactic for forming the eight-membered ring, a synthetic plan was devised that would allow modular construction of aldehyde **28**, so that both (+)-**4** and 12-*epi*-**4** could be prepared. It was anticipated that **28** could arise from the bifunctional hydrindanone fragment **30** by crotylation with either *Z*- or *E*-boronic acid **31**.[21] Hydrindanone enal **30** was mapped back to cyclohexenone **32**, available in one step from (+)-*trans*-dihydrocarvone.[22]

Figure 1.9 *18-Step total synthesis of (+)-pleuromutilin*

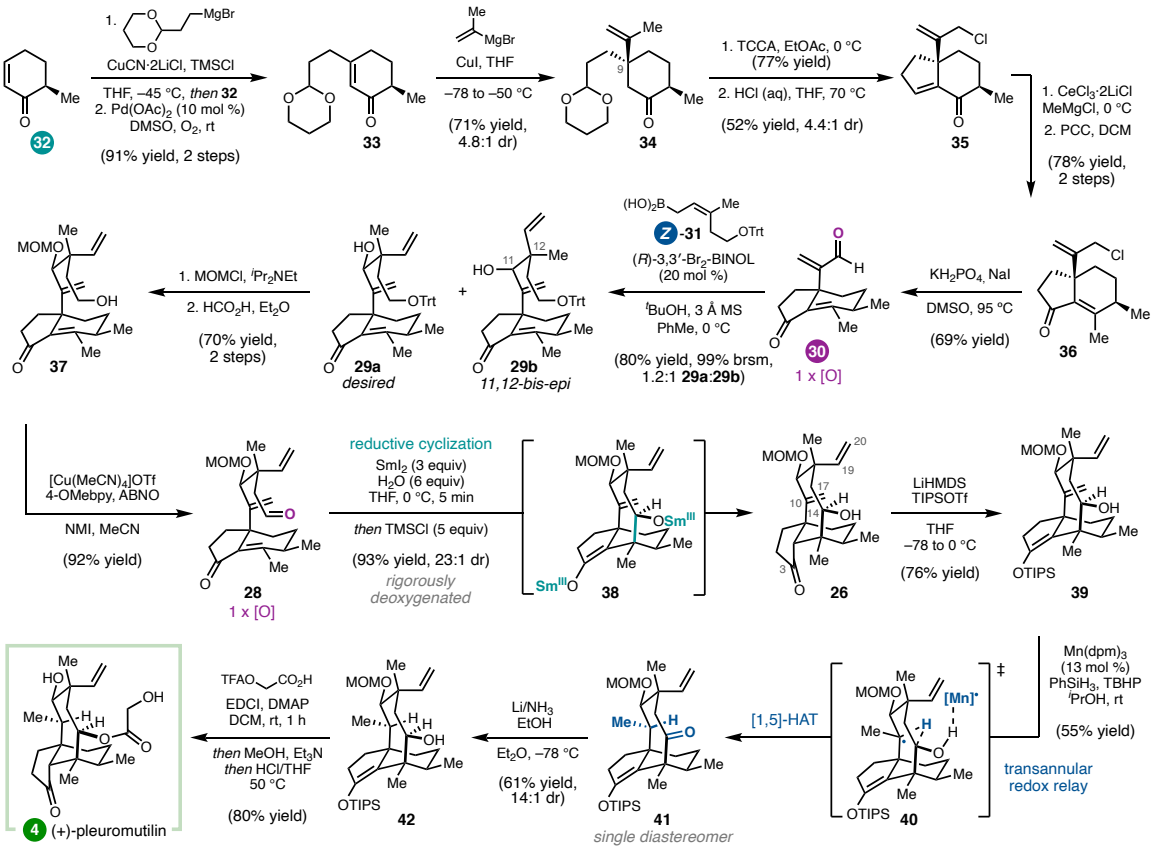

In the forward direction, ketone **34**, bearing a C9 quaternary center, was prepared via sequential conjugate additions (Figure 1.9). Allylic chlorination of the *iso*-propenyl group of **34** was performed prior to intramolecular aldol condensation in order to avoid a

competing, undesired Prins-type cyclization. Ketone **35** could be elaborated to enal **30** in three additional steps.

To complete the first of two key bond-forming steps, selective *syn*-crotylation with boronic acid *Z*-**31** gave desired diastereomer **29a** after chromatographic separation. Unfortunately, despite the use of a chiral BINOL catalyst,[23] high diastereoface selectivity for addition to the aldehyde was not able to be obtained. Nonetheless, the required diastereomer (**29a**) could be elaborated in three steps to aldehyde **28**. To form the eight-membered ring, a freshly prepared SmI_2 solution was added dropwise to **28**; quenching of presumed Sm-enolate **38** with trimethylsilyl chloride then delivered tricycle **26** as a separable 23:1 mixture of diastereomers. Substantial optimization determined that rigorously anaerobic conditions were critical for minimizing byproduct formation and that addition of water was important for high diastereoselectivity.

At this stage, completion of the synthesis hinged upon selective hydrogenation of the C10 *exo*-methylene in the presence of the C19 vinyl group. It was hypothesized that metal-catalyzed hydrogen atom transfer (MHAT) reduction might provide a solution, wherein the thermodynamic preference for formation of a tertiary carbon-centered radical could be leveraged. Indeed, chemoselective reduction of the exocyclic C10–C17 olefin was achieved; however, this reduction was accompanied by unanticipated C14 oxidation. Deuterium labeling experiments revealed that this reaction proceeds by a transannular [1,5]-HAT redox relay, thermodynamically driven by formation of the C14 ketone. By protecting the C3 ketone of **26** as a silyl enol ether prior to the MHAT redox relay, the C14 ketone of **41** could be reduced using dissolving metal conditions while preserving the ketone oxidation state at C3. Finally, acylation followed by global deprotection under

acidic conditions afforded (+)-pleuromutilin (**4**) in 18 steps in the longest linear sequence.[2]

Figure 1.10 *18-Step total synthesis of (+)-12-*epi*-pleuromutilin*

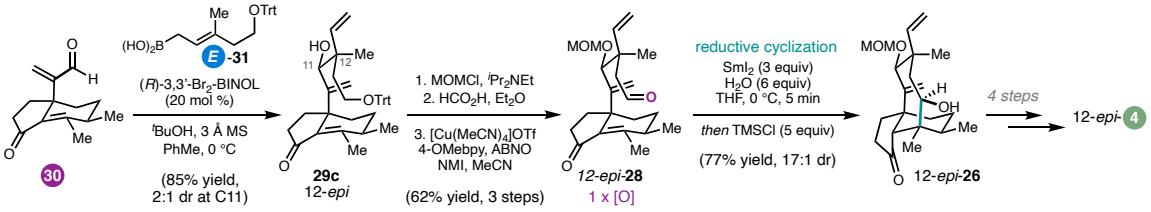

An advantage of this modular approach was the ability to readily prepare the 12-*epi*-**4** framework by varying the relative configuration of cyclization substrates at C12 (Figure 1.10). To this end, enal **30** was crotylated with *E*-**31** to deliver **29c**, which was elaborated to 12-*epi*-**28** without difficulty. Exposure of 12-*epi*-**28** to the optimal SmI_2 cyclization conditions furnished 12-*epi*-**26**, then advanced via the previously developed 4-step sequence to complete the synthesis of 12-*epi*-**4**.

The brevity and modularity of these syntheses, enabled by the unique ability of radical cyclizations to overcome the challenges that dissonant charge affinity patterns pose to standard bond constructions, are anticipated to facilitate preparation of new pleuromutilin antibiotics.

1.3 COMPCOMPLEX OXIDATION TOPOLOGY

1.3.1 *Ryanodane Diterpenes*

A classic example of how natural products can impact understanding of biology is the story of (+)-ryanodine. (+)-Ryanodine (**5**) is a highly oxidized diterpene isolated from the tropical shrub *Ryania speciose* Vahl.[23] Investigation of ryanodine's insecticidal properties ultimately led to the purification and characterization of intracellular Ca^{2+} ion

channels now known as the ryanodine receptors (RyRs),[24,25] which are involved in a number of signal transduction processes. Whereas both **5** and its hydrolysis product (+)-ryanodol (**43**) bind insect RyRs,[26] **43** exhibits significantly lower affinity for mammalian receptors.[27] In addition, structurally related diterpenes that vary in peripheral oxidation, including (+)-20-deoxyspiganthine (**44**), have also been identified as RyR modulators.[28]

Due to their biological importance, ryanodanes have been the focus of total synthesis[29,30] and medicinal chemistry[30,31] efforts for several decades. However, at the outset of these studies, there were no completed total syntheses of ryanodine, due in part to the challenges associated with introduction of the pyrrole-2-carboxylate at the C3 alcohol of ryanodol (**43**). With the long-term goal of developing new probes of RyR function, a synthetic platform was devised for the preparation of (+)-**5** and related congeners (i.e., (+)-**44**).

Figure 1.11 *Retrosynthetic analysis of ryanodane diterpenes*

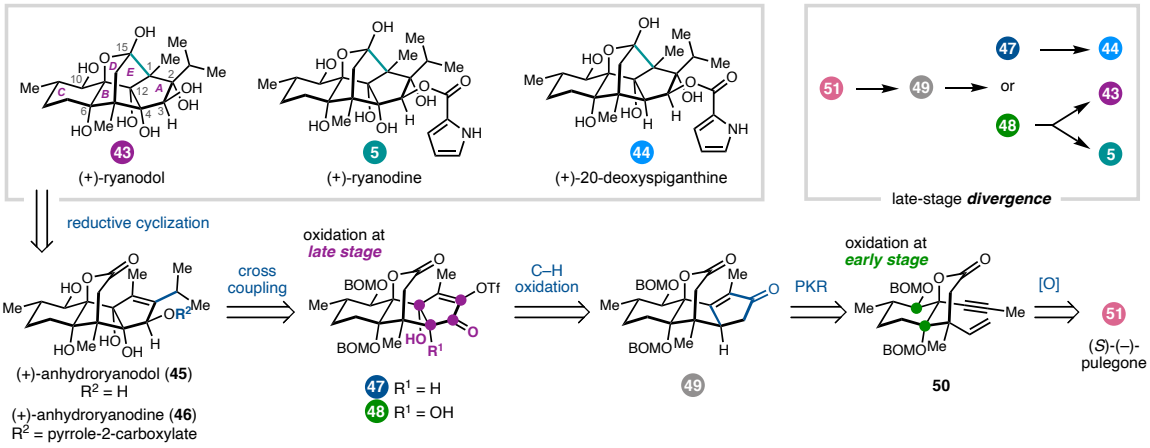

Initial efforts focused on the preparation of (+)-**43**, with the idea that the synthetic strategy could be applied to (+)-**5** and other ryanodanes (Figure 1.11).[32,33,34] Inspiration was drawn from early relay studies by Deslongchamps and coworkers, which established that the C1–C15 bond of the bridging E ring could be formed via epoxidation of **45**

followed by reductive cyclization.[32] With (+)-anhydroryanodol (**45**) as a slightly simpler target, the strategy was directed by the dense oxidation of the tetracyclic core. It was hypothesized that an A-ring cyclopentenone, such as that in **49**, could undergo sequential oxidation in the final steps of the synthesis to install the C3 alcohol and the *syn*-C4–C12-diol with the appropriate stereochemistry. In contrast, the C-ring oxidation could be incorporated early in the synthesis while assembling the carbon framework. With this goal in mind, an intramolecular Pauson–Khand reaction (PKR)[35] was identified as a key tactic to prepare cyclopentenone **49**. The requisite enyne (**50**) was mapped back to (*S*)-(–)-pulegone (**51**), with the expectation that sequential oxidation α to the ketone could be used to install the C6 and C10 alcohols.

Studies began with the oxidation of (*S*)-(–)-pulegone (**51**, Figure 1.12). Although a multistep sequence to **53** via known pulegone oxide was initially envisioned, it was ultimately found that treatment of **51** with excess KHMDS followed by oxaziridine **52** resulted in dihydroxylation to form **53** as the major diastereomer. Further mechanistic investigations are required, but preliminary studies suggest that the reaction proceeds first by generation of the thermodynamic potassium dienolate, which upon reaction with **52** gives rise to the C6 tertiary alkoxide as a mixture of diastereomers.[36] A second enolization and oxidative trapping gives rise to α,α′-diol **53** in 40–50% yield following silica gel chromatography. In this single transformation, a key building block is accessed with the complete C-ring functionality found in ryanodol and ryanodine.

Following protection of the alcohols, the D ring was constructed by a four-step sequence involving 1,2-addition of prop-1-yn-1-yl magnesium bromide followed by ozonolytic olefin cleavage to afford ketone **55**. A second 1,2-addition and subsequent Ag-

catalyzed cyclization/elimination cascade[37] then gave α,β-unsaturated lactone **56**. The critical all-carbon quaternary center was formed as a single diastereomer by 1,4-addition of a vinyl cuprate reagent, giving **50**. Pauson–Khand cyclization with catalytic $[RhCl(CO)_2]_2$ under an atmosphere of carbon monoxide (CO) provided cyclopentenone **49** as a single diastereomer.[38]

Figure 1.12 *15-Step total synthesis of (+)-ryanodol*

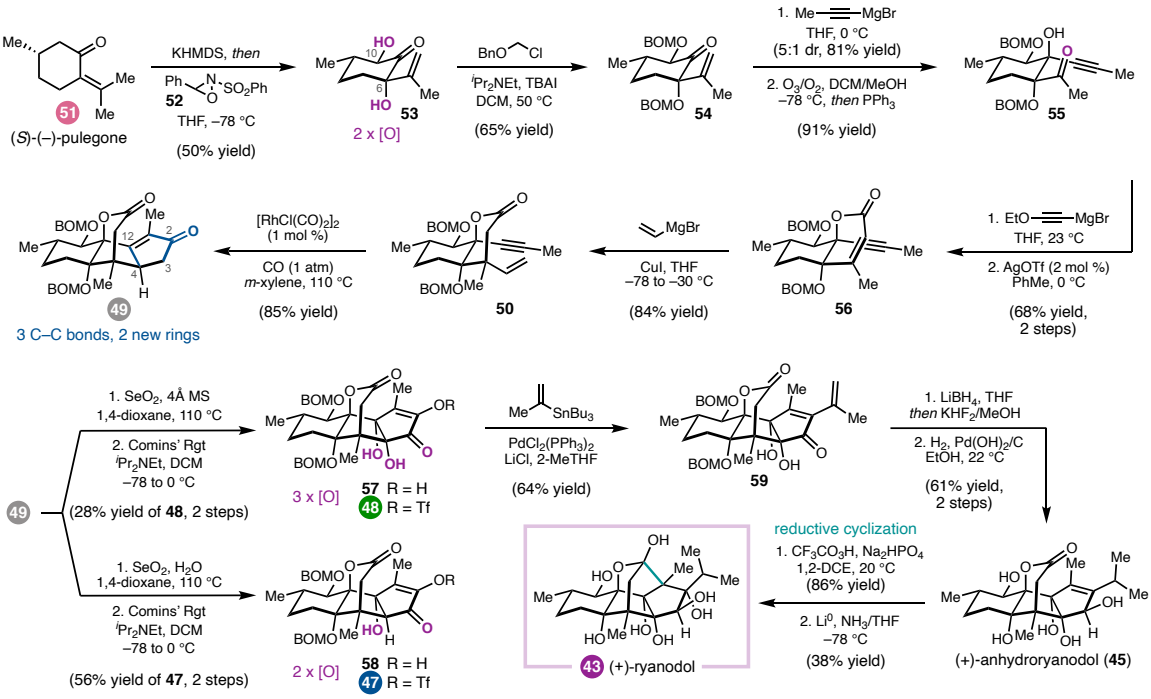

Having identified a concise route to tetracycle **49**, the remaining task was the challenging introduction of the alcohols at C3, C4, and C12, with the C4 alcohol expected to be the most challenging of the three. Initially, conditions were investigated for allylic oxidation at C4; however, this proved unfruitful and led to the pursuit of SeO_2-mediated α-oxidation of the C2 ketone.[39] Surprisingly, treatment of **49** with SeO_2 and K_3PO_4 in refluxing dioxane resulted in the isolation of hydroxyenone **58**, wherein the presumed intermediate enediketone underwent hydration at C12. Careful analysis of the

reaction mixtures indicated the presence of a minor side-product assigned the structure of **57**, a compound which had undergone further oxidation at C4. Although the yield was very low (<5%), it was recognized that this remarkable transformation installs the oxygen atoms at C3, C4, and C12, as well as a functional group handle for incorporation of the C2-*iso*-propyl group, all in a single step. As result, improvement to the yield was sought, and ultimately heating **49** with excess SeO_2 in rigorously anhydrous 1,4-dioxane gave increased amounts of **57**, which could be isolated as enol triflate **48** in 28% yield over the two steps. Alternatively, oxidation of **49** with SeO_2 and 10 equiv water in 1,4-dioxane, followed by triflation, gave **47** in 56% yield.

To complete the synthesis of (+)-**43**, enol triflate **48** was submitted to Pd-catalyzed Stille cross-coupling, ketone reduction, and hydrogenation to deliver (+)-anyhdyroryanodol (**45**). In slight modification of the reported protocol,[32] treatment of **45** with freshly prepared trifluoroperacetic acid cleanly afforded the *epi*-anhydroryanodol epoxide, which could be subjected to Li in NH_3 to effect reductive cyclization to (+)-ryanodol (**43**).[3] With only 15 steps, this synthesis represents a ca. 50% reduction in length compared to previous syntheses.[32,33]

Given the known challenge associated with preparing ryanodine by site-selective C2 acylation of **43**, the synthetic strategy to **5** called for departure from the ryanodol end game, such that the pyrrole 2-carboxalate could be introduced selectively without extensive additional protecting group manipulations.[33a,c;34,40] Moreover, it was anticipated that dioxidation product **47** could be used to prepare the related natural product 20-deoxyspiganthine. Although there was some uncertainty as to whether the pyrrole 2-carboxalate could survive the final reductive cyclization, anhydroryanodol derivatives **61**

(Figure 1.13) and **68** (Figure 1.14) were nonetheless identified as potential candidates for acylation.

Figure 1.13 *18-Step total synthesis of (+)-ryanodine*

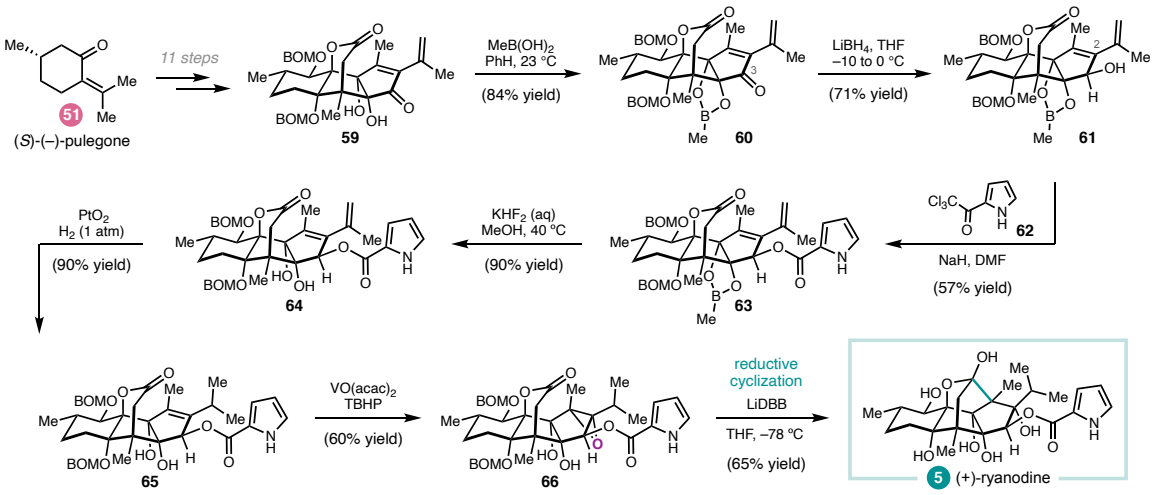

The synthesis of (+)-**5** commenced with diol **59**, which was strategically protected as a dioxaborinane (Figure 1.13). Reduction of the C3-ketone furnished **61**, bearing a single unprotected alcohol. A survey of standard acylating reagents derived from pyrrole-2-carboxylic acid failed to deliver pyrrole ester **63**; however, deprotonation of alcohol **61** before addition of trichloroketone **62** successfully provided **63**. This reaction is noteworthy: efforts to perform the acylation on a compound bearing an *iso*-propyl, instead of *iso*-propenyl, substituent at C2 were unsuccessful. Subsequent deprotection, hydrogenation, and hydroxyl-directed epoxidation revealed **66**. Whereas the use of Li/NH_3, the conditions employed for the synthesis of ryanodol, resulted in reductive cyclization with concomitant deacylation, the use of lithium di-*tert*-butylbiphenylide (LiDBB) in THF effected C–C bond formation and alcohol debenzylation to provide (+)-ryanodine (**5**) in 65% yield.[35]

A similar sequence was used to elaborate alcohol **67** to 20-deoxyspiganthine (**44**, Figure 1.14). In this case, the C12 alcohol was protected as a TMS ether prior to reduction of the C3 ketone. Despite the similarity of **68** to **61**, this acylation required further optimization of the reaction conditions in order to minimize non-productive translactonization. Ultimately, **68** was treated with excess KHMDS to enolize the lactone and prevent translactonization; while this enabled acylation of the C3 alcohol with pyrrole **69**, α-chlorination of the lactone was also observed. Radical dechlorination of **70** afforded lactone **71**, which was uneventfully advanced to (+)-20-deoxyspiganthine (**44**) by hydrogenation, epoxidation, and reductive cyclization.[35] This represents the first total synthesis of a spiganthine-type natural product.

Figure 1.14 *19-Step total synthesis of (+)-20-deoxyspiganthine*

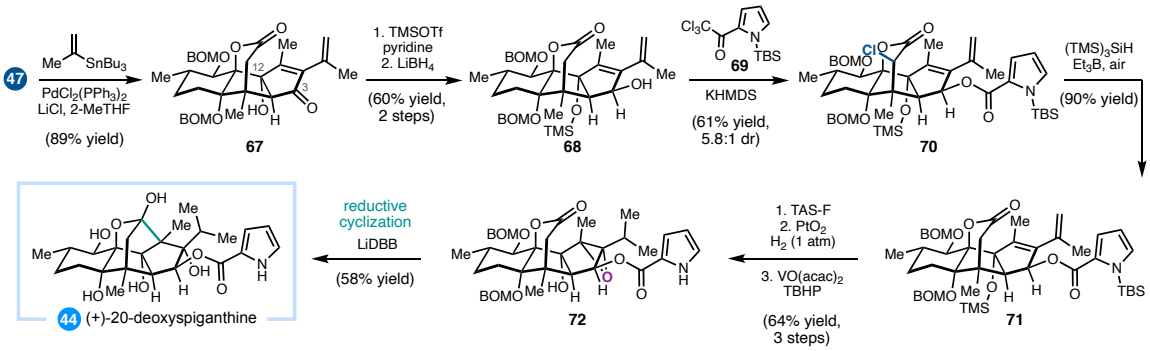

Taken together, these ryanodane studies highlight how managing formation of C–C and C–O bonds to introduce functionality at the correct oxidation level can minimize protecting group adjustments and lead to concise syntheses.

1.3.2 *Isoryanodane Diterpenes*

Having established a synthetic strategy to prepare several ryanodane natural products, attention was turned to a related family of targets: the isoryanodanes. The

isoryanodanes possess a 5-6-5 ABC ring system instead of the 5-5-6 system found in the ryanodanes but bear a similar, dense oxidation pattern. Although it has not been conclusively established, it seems likely that these compounds are biosynthetically related. One interesting divergence is that none of the isoryanodanes isolated to date possess a pyrrole-2-carboxylate ester like that found in ryanodine, although many retain potent insecticidal properties. For example, (+)-perseanol (**6**) [41] displays potent antifeedant activity with low toxicity to mammalian cells,[42] as do related isoryanodane diterpenes.[43] This has raised the question as to whether the target of these compounds is indeed the insect RyR or whether they act through a distinct mode-of-action. Perseanol is decorated by six free hydroxyl groups around a highly caged pentacyclic core that includes a bridging 7-membered lactol. Prior to these studies, there was a single report describing an approach to the complex framework but no completed syntheses.[44] Inspired by the potential to further investigate isoryanodane mode-of-action, a convergent synthesis of (+)-**6** was developed.[45]

Figure 1.15 *Retrosynthetic analysis of (+)-perseanol*

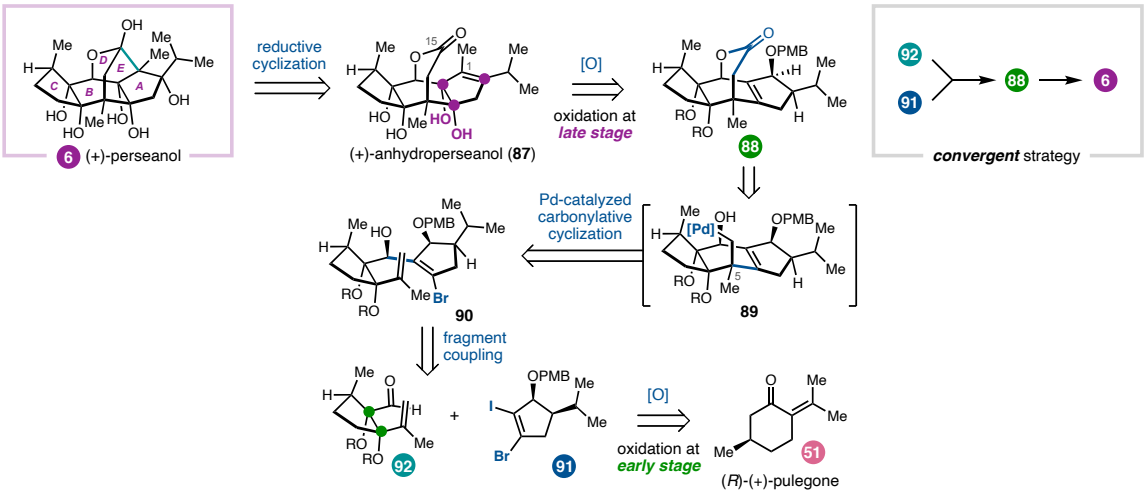

Guided by the approach to ryanodine, a late-stage reductive cyclization was envisioned that could be used to form the C1–C15 bond, leading to retrosynthetic simplification of **6** to anhydroperseanol (**87**, Figure 1.15). Although a Pauson–Khand approach was initially pursued to prepare the carbon framework of anhydroperseanol, this led to challenges in forming the 7-membered lactone-containing enyne. These challenges led us to a revised synthetic strategy. Analysis of the oxidation patterns in **87** suggested that the A–B ring fusion diol could be accessed from tetracyclic alkene **88**, whereas the B–C ring fusion diol might be introduced early in the synthesis. Tetracyclic lactone **88** was dissected into two fragments that could be joined in two C–C bond-forming steps. First, 1,2-addition of a metallated fragment derived from **91** into aldehyde **92** was envisioned. Second, the resulting alkenyl bromide (**90**) could undergo an intramolecular Pd-catalyzed carbopalladation/carbonylation cascade to forge the central 7-membered lactone. To access the enantioenriched fragments required for a convergent fragment coupling, enal **92** was expected to be prepared from (*R*)-(+)-pulegone (**51**) and vicinal dihalide **91** from commercially available 3-ethoxycyclopent-2-en-1-one (**99**).

Figure 1.16 *Preparation of the C-ring fragment*

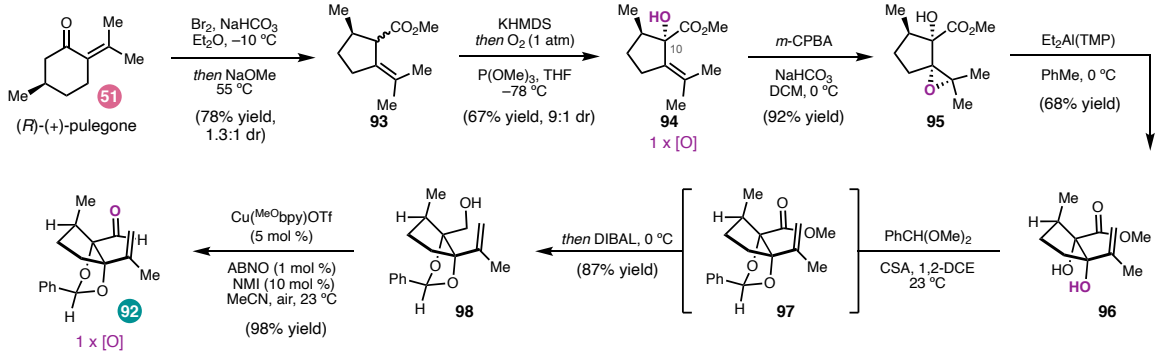

In the forward sense, the C-ring fragment (**92**) was prepared by known Favorskii rearrangement[46] of **51** followed by diastereoconvergent α-hydroxylation to yield **94**

(Figure 1.16). Hydroxyl-directed epoxidation and isomerization then provided *syn*-diol **96**. Through this four-step sequence, the B–C ring fusion diol was efficiently introduced at the beginning of the synthesis with the correct relative stereochemistry. Diol **96** could be elaborated in two additional steps to alkenyl aldehyde **92**.

Figure 1.17 *Preparation of the A-ring fragment*

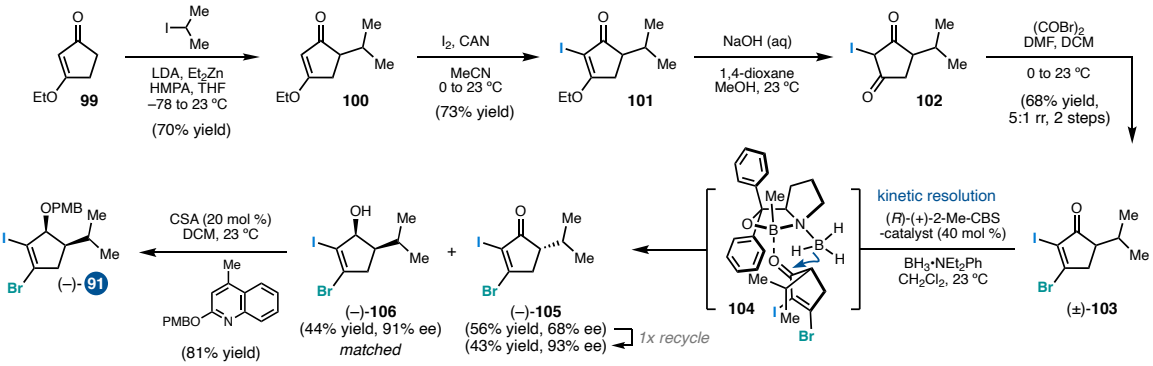

Synthesis of the A-ring fragment (**91**) began with alkylation of the zinc enolate of vinylogous ester **99** (Figure 1.17). An iodination/hydrolysis sequence provided diketone **102**, which was immediately brominated to yield bromoiodocyclopentenone **103**. Finally, an enantioselective Corey–Bakshi–Shibata (CBS) reduction[47] of (±)-**103** resulted in a kinetic resolution that provided alcohol (–)-**106** in 91% enantiomeric excess, which was protected to furnish dihalide fragment **91**.

With both fragments in hand, a two-step annulation strategy was investigated to forge the tetracyclic ring system. Selective lithiation of iodide **91** and addition to aldehyde **92** provided secondary alcohol **90** in good yield but modest diastereoselectivity (Figure 1.18). To close the central B ring, a carbopalladation/carbonylation cascade was investigated, with the goal of forging two C–C bonds and setting the all-carbon quaternary center in a single step. This reaction required extensive optimization to identify conditions that favored formation of the seven-membered lactone in preference

to the five-membered lactone accessible via competitive direct carbonylation of the alkenyl bromide. In particular, it was important to maintain a low concentration of CO in solution to avoid inhibition of alkenyl bromide oxidative addition and to favor alkene insertion prior to carbonylation. Ultimately, use of *N*-formylsaccharin with KF as an activator[48] and 50 mol% $Pd(PPh_3)_4$ proved optimal; under these conditions, the bridging lactone **88** could be formed in 57% yield as a single diastereomer.

Figure 1.18 *16-Step total synthesis of (+)-perseanol*

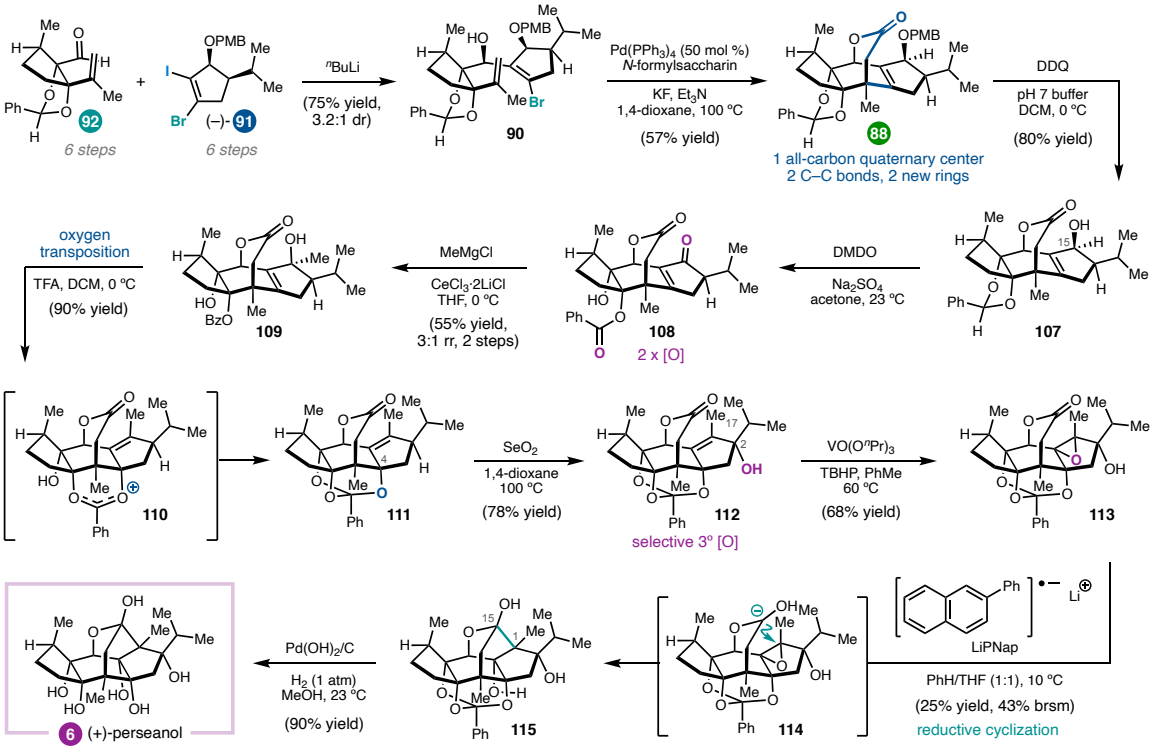

To complete the synthesis, the tetrasubstituted allylic alcohol needed to be transformed into the A–B ring fusion diol. To this end, PMB deprotection of **88** followed by treatment with dimethyl dioxirane (DMDO) was found to deliver the C15 ketone, in addition to unexpected benzylidene acetal oxidation. This transformation had not been a part of the initial plan; we nonetheless continued with efforts to elaborate towards **6**.

Following 1,2-addition of methyl Grignard to hydroxybenzoate **108**, it was discovered that diol **109** could be converted to orthobenzoate **111** by treating with trifluoroacetic acid, presumably proceeding through dioxolenium ion **110**. This three-step sequence, although outside of the original synthetic design, allowed us to repurpose the benzylidene acetal from a diol protecting group to an anchimeric directing group. Having enabled installation of the C4 tertiary alcohol, it resumed the role as an alcohol protecting group, now in the form of an orthobenzoate. This series of transformations illustrates how some of the most strategic reaction sequences arise from leveraging the emergent reactivity of the molecule, rather than strictly adhering to a preconceived synthetic design.

Tetracyclic alkene **111** was found to undergo selective allylic oxidation of the tertiary C–H bond at C2 to give allylic alcohol **112**. Again, an opportunity to revise the synthetic plan arose. Although epoxidizing anhydroperseanol (**87**) in order to execute a reductive cyclization analogous to those employed in the syntheses of ryanodine and ryanodol had been initially envisioned, it was recognized that the synthesis could be streamlined by instead preparing the isomeric epoxide **113**. This type of reductive cyclization was unprecedented; however, given that **112** could be stereoselectively converted to **113** in good yield, it seemed worthwhile to pursue.

Extensive investigation of a variety of reductants revealed that lithium 2-phenylnaphthalenide in THF/benzene effected the reductive cyclization of **113** to construct the C1–C15 bond and deliver **115** in 25% yield. Interestingly, C2-des-*iso*-propyl-**113** undergoes reductive cyclization in >50% yield (not shown), indicating that the steric bulk of the *iso*-propyl substituent likely slows down the rate of C–C bond formation. Final hydrogenolysis of the orthobenzoate afforded (+)-perseanol (**6**).[4] The

successful first total synthesis of (+)-**6** in 16 linear steps testifies to the power of convergent fragment couplings; additionally, the opportunistic formation of the A–B ring fusion diol illustrates that strategic redox planning can enable fortuitous discoveries to drive synthetic efficiency.

1.4 CONCLUDING REMARKS

The preceding sections detail several total syntheses of diterpene natural products. In these examples, synthetic planning was guided by target structures, with bond-forming tactics chosen to leverage inherent functional group relationships and their charge affinity patterns in order to minimize redundant changes to carbon oxidation states. In addition, careful choreography of C–C and C–O bond construction allowed strategic introduction of oxidation, thereby reducing synthetic manipulations ancillary to the direct assembly of the natural product.

At the broader level, these intellectual advancements provide a conceptual framework that has motivated our efforts to develop new strategies and methodologies for the synthesis of additional natural products. In Chapter 3, we explore in greater detail unusual oxidative reactivity (see Fig. 1.12) as methods for the simultaneous installation of multiple C–O bonds in natural product-like scaffolds. In the following chapters, we turn to tactics for strategic C–C bond formation complementary to the methods presented above. Specifically, we discuss reductive cross-coupling reactions (introduced in Chapter 2), which we anticipated to be particularly effective for carbocycle construction and enable efforts to synthesize the rearranged isoryanodane diterpene (+)-cassiabudanol A (Chapter 4), as well as the macrocyclic cylindrocyclophane natural products (Chapter 5).

1.5 REFERENCES

(1) Breitmaier, E. *Terpenes: Flavors, Fragrances, Pharmaca, Pheromones*; John Wiley & Sons, 2006.

(2) (a) Corey, E. J.; Cheng, X.-M. *The Logic of Chemical Synthesis*; Wiley, 1989. (b) Evans, D. A.; Andrews, G. C. Allylic Suloxides: Useful intermediates in orgnic Synthesis. *Acc. Chem. Res.* **1971**, *7*, 147–155. (c) Evans, D. A. *An Organizational Format for the Classification of Functional Groups. Applications to the Construction of Difunctional Relationships.* (c) Seebach, D. Methods of Reactivity Umpolung. *Angew. Chem. Int. Ed.* **1979**, *18* (4), 239–258. (d) Hendrickson, J. B. Systematic Characterization of Structures and Reactions for Use in Organic Synthesis. *J. Chem. Soc.* **1971**, *93* (25), 6847–6854.

(3) Koehn, F. E.; Carter, G. T. The Evolving Role of Natural Products in Drug Discovery. *Nat. Rev. Drug Discov.* **2005**, *4* (3), 206–220.

(4) (a) Molander, G. A.; Harris, C. R. Sequencing Reactions with Samarium(II) Iodide. *Chem. Rev.* **1996**, *96* (1), 307–338. (b) Edmonds, D. J.; Johnston, D.; Procter, D. J. Samarium(II)-Iodide-Mediated Cyclizations in Natural Product Synthesis. *Chem. Rev.* **2004**, *104* (7), 3371–3404.

(5) (a) Fukuzawa, S.-I.; Nakanishi, A.; Fujinami, T.; Sakai, S. Reductive Coupling of Ketones or Aldehydes with Electron-deficient Alkenes Promoted by Samarium di-iodide. *J. Chem. Commun.* **1986**, 624–625. (b) Enholm, E. J.; Trivellas, T. Lanthanide Induced Intramolecular Coupling of Aldehydes and Ketones with Electron-Deficient Olefins. *Tetrahedron Lett.* **1989**, *30*, 1063–1066. (c) Helm, M.

D.; Sucunza, D.; Da Silva, M.; Helliwell, M.; Procter, D. J. SmI_2-Mediated Dialdehyde Cyclization Cascades. *Tetrahedron Lett.* **2009**, *50*, 3224–3226.

(6) Sun, H.-D.; Huang, S.-X.; Han, Q.-B. Diterpenoids from *Isodon* species and their biological activities. *Nat. Prod. Rep.* **2006**, *23*, 673–698.

(7) (a) Han, Q.-B.; Cheung, S.; Tai, J.; Qiao, C.-F.; Song, J.-Z.; Tso, T.-F.; Sun, H.-D.; Xu, H.-X. Maoecrystal Z, a Cytotoxic Diterpene from *Isodon eriocalyx* with a Unique Skeleton. *Org. Lett.* **2006**, *8* (21), 4727–4730. (b) Node, M.; Sai, M.; Fuji, K.; Fujita, E.; Shingu, T.; Watson, W. H.; Grossie, D. Three New Anti-Tumor Diterpenoids, Trichorabdals A, C, And D. *Chem. Lett.* **1982**, *11* (12), 2023–2026. (c) Fujita, T.; Takeda, Y.; Shingu, T. Longikaurin C, D, E and F; New Antibacterial Diterpenoids from *Rabdosia longituba*. *Heterocycles* **1981**, *16* (92), 227–230.

(8) Kawaide, H.; Imai, R.; Sassa, T.; Kamiya, Y. *ent*-Kaurene Synthase from the Fungus *Phaeosphaeria* sp. L487 cDNA Isolation, Characterization, and Bacterial Expression of a Bifunctional Diterpene Cyclase in Fungal Gibberellin Biosynthesis. *J. Biol. Chem.* **1997**, *272* (35), 21706–21712.

(9) (a) Fuji, K.; Node, M.; Sai, M.; Fujita, E.; Takeda, S.; Unemi, N. Terpenoids. LIII.: Antitumor Activity of Trichorabdals and Related Compounds. *Chem. Pharm. Bull.* **1989**, *37* (6), 1472–1476. (b) Zhao, W.; Pu, J.-X.; Du, X.; Su, J.; Li, X.-N.; Yang, J.-H.; Xue, Y.-B.; Li, Y.; Xiao, W.-L.; Sun, H.-D. Structure and Cytotoxicity of Diterpenoids from *Isodon adenolomus*. *J. Nat. Prod.* **2011**, *74* (5), 1213–1220.

(10) Yeoman, J. T. S.; Cha, J. Y.; Mak, V. W.; Reisman, S. E. A Unified Strategy for the Synthesis of (−)-Maoecrystal Z, (−)-Trichorabdal A, and (−)-Longikaurin E.

Tetrahedron **2014**, *70* (27), 4070–4088.

(11) Fujita, E.; Fuji, K.; Sai, M.; Node, M.; Watson, W. H.; Zabel, V. The structure of trichorabdal B and its transformation into a novel skeleton; *X*-ray crystal structures. *J. Chem. Soc. Chem. Commun.* **1981**, *17*, 899–900.

(12) Cha, J. Y.; Yeoman, J. T. S.; Reisman, S. E. A Concise Total Synthesis of (−)-Maoecrystal Z. *J. Am. Chem. Soc.* **2011**, *133* (38), 14964–14967.

(13) (a) RajanBabu, T. V.; Nugent, W. A. *J. Am. Chem. Soc.* **1989**, *111*, 4525. (b) RajanBabu, T. V.; Nugent, W. A. *J. Am. Chem. Soc.* **1994**, *116*, 986. (c) Gansäauer, A.; Pierobon, M.; Bluhm, H. Catalytic, Highly Regio- and Chemoselective Generation of Radicals from Epoxides: Titanocene Dichloride as an Electron Transfer Catalyst in Transition Metal Catalyzed Radical Reactions. *Angew. Chem. Int. Ed.* **1998**, 37 (1), 101–103. (d) Gansäuer, A.; Bluhm, H.; Rinker, B.; Narayan, S.; Schick, M.; Lauterbach, T.; Pierobon, M. Reagent-Controlled Stereoselectivity in Titanocene-Catalyzed Epoxide Openings: Reductions and Intermolecular Additions to *α*,*β*-Unsaturated Carbonyl Compounds. *Chem. Eur. J.* **2003**, *9* (2), 531–542.

(14) Yeoman, J. T. S.; Mak, V. W.; Reisman, S. E. A Unified Strategy to Ent-Kauranoid Natural Products: Total Syntheses of (−)-Trichorabdal A and (−)-Longikaurin E. *J. Am. Chem. Soc.* **2013**, *135* (32), 11764–11767.

(15) (a) Ito, Y.; Aoyama, H.; Hirao, T.; Mochizuki, A.; Saegusa, T. Cyclization reactions via oxo-.pi.-allylpalladium(II) intermediates. *J. Am. Chem. Soc.* **1979**, *101* (2), 494–496. (b) Kende, A. S.; Roth, B.; Sanfilippo, P. J. Facile, palladium(II)-mediated

synthesis of bridged and spirocyclic bicycloalkenones. *J. Am. Chem. Soc.* **1982**, *104*, 1784–1785.

(16) (a) Kavanagh, F.; Hervey, A.; Robbins, W. J. Proc. Natl. Acad. Sci. U. S. A. 1951, 37, 570. (b) Birch, A. J.; Holzapfel, C. W.; Rickards, R. W. The structure and some aspects of the biosynthesis of pleuromutilin. *Tetrahedron* **1966**, *22* (Suppl. 8), 359–387. (c) Poulsen, S. M.; Karlsson, M.; Johansson, L. B.; Vester, B. The pleuromutilin drugs tiamulin and valnemulin bind to the RNA at the peptidyl transferase centre on the ribosome. *Mol. Microbiol.* **2001**, *41* (5), 1091−1099.

(17) (a) Brooks, G.; Burgess, W.; Colthurst, D.; Hinks, J. D.; Hunt, E.; Pearson, M. J.; Shea, B.; Takle, A. K.; Wilson, J. M.; Woodnutt, G. Pleuromutilins. Part 1: The Identification of Novel Mutilin 14- Carbamates. *Bioorg. Med. Chem.* **2001**, *9* (5), 1221−1231. (b) Rittenhouse, S.; Biswas, S.; Broskey, J.; McCloskey, L.; Moore, T.; Vasey, S.; West, J.; Zalacain, M.; Zonis, R.; Payne, D. Selection of Retapamulin, a Novel Pleuromutilin for Topical Use. *Antimicrob. Agents Chemother.* **2006**, *50* (11), 3882−3885.

(18) Thirring, K.; Heilmayer, W.; Riedl, R.; Kollmann, H.; Ivezic- Schoenfeld, Z.; Wicha, W.; Paukner, S.; Strickmann, D. WO2015110481A1, July 30, 2015.

(19) Farney, E. P.; Feng, S. S.; Schäfers, F.; Reisman, S. E. Total Synthesis of (+)-Pleuromutilin. *J. Am. Chem. Soc.* **2018**, *140* (4), 1267–1270.

(20) (a) Gibbons, E. G. Total synthesis of (+)-pleuromutilin. *J. Am. Chem. Soc.* **1982**, *104* (6), 1767–1769. (b) Boeckman, R. K., Jr.; Springer, D. M.; Alessi, T. R. Synthetic studies directed toward naturally occurring cyclooctanoids. 2. A

stereocontrolled assembly of (+)-pleuromutilin via a remarkable sterically demanding oxy-Cope rearrangement. *J. Am. Chem. Soc.* **1989**, *111* (21), 8284–8286. (c) Helm, M. D.; Da Silva, M.; Sucunza, D.; Findley, T. J. K.; Procter, D. J. A dialdehyde cyclization cascade: An approach to pleuromutilin. *Angew. Chem. Int. Ed.* **2009**, *48* (49), 9315–9317. (d) Fazakerley, N. J.; Helm, M. D.; Procter, D. J. Total Synthesis of (+)-Pleuromutilin. *Chem. Eur. J.* **2013**, *19* (21), 6718–6723. (e) Murphy, S. K.; Zeng, M.; Herzon, S. B. A modular and enantioselective synthesis of the pleuromutilin antibiotics. *Science* **2017**, *356* (6341), 956–959. (f) Zeng, M.; Murphy, S. K.; Herzon, S. B. Development of a Modular Synthetic Route to (+)-Pleuromutilin, (+)-12-epi-Mutilins, and Related Structures. *J. Am. Chem. Soc.* **2017**, *139* (45), 16377–16388.

(21) (a) Lou, S.; Moquist, P. N.; Schaus, S. E. Asymmetric allylboration of ketones catalyzed by chiral diols. *J. Am. Chem. Soc*. **2006**, *128* (39), 12660–12661. (b) Alam, R.; Vollgraff, T.; Eriksson, L.; Szabó, K. L. Synthesis of adjacent quaternary stereocenters by catalytic asymmetric allylboration. *J. Am. Chem. Soc.* **2015**, *137* (35), 11262–11265.

(22) White, J. D.; Grether, U. M.; Lee, C. S. (R)-(+)-3, 4-Dimethylcyclohex-2-en-1-one: ((R)-(+)-3, 4-Dimethyl-2-cyclohexen-1-one). *Org. Synth.* **2005**, *82*, 108–114.

(23) (a) Rogers, E. F.; Koniuszy, F. R.; Shavel, J.; Folkers, K. Plant Insecticides. I. Ryanodine, A New Alkaloid from Ryania Speciosa Vahl. *J. Am. Chem. Soc.* **1948**, *70* (9), 3086−3088. (b) Wiesner, K.; Valenta, Z.; Findlay, J. A. The structure of ryanodine. *Tetrahedron Lett.* **1967**, *8* (3), 221–223.

(24) (a) Pessah, I. N.; Waterhouse, A. L.; Casida, J. E. The calcium-ryanodine receptor complex of skeletal and cardiac muscle. *Biochem. Biophys. Res. Commun.* **1985**, *128* (1), 449−456. (b) Inui, M.; Saito, A.; Fleischer, S. solation of the ryanodine receptor from cardiac sarcoplasmic reticulum and identity with the feet structures. *J. Biol. Chem.* **1987**, *262* (32), 15637−15642.

(25) (a) *Ryanodine Receptors: Structure, Function and Dysfunction in Clinical Disease*; Wehrens, X. H. T., Marks, A. R., Eds.; Developments in Cardiovascular Medicine; Springer US, 2005. (b) Lanner, J. T. *Ryanodine Receptor Physiology and Its Role in Disease. In Calcium Signaling*; Islam, M. S., Ed.; Advances in Experimental Medicine and Biology; Springer: Dordrecht, The Netherlands, 2012.

(26) (a) Meissner, G. Ryanodine activation and inhibition of the Ca2+ release channel of sarcoplasmic reticulum. *J. Biol. Chem.* **1986**, *261* (14), 6300−6306. (b) Meissner, G.; El-Hashem, A. Ryanodine as a functional probe of the skeletal muscle sarcoplasmic reticulum Ca 2+ release channel. *Mol. Cell. Biochem.* **1992**, *114* (1), 119−123.

(27) Sutko, J. L.; Airey, J. A.; Welch, W.; Ruest, L. The pharmacology of ryanodine and related compounds. *Pharmacol. Rev.* **1997**, *49* (1), 53−98.

(28) (a) Achenbach, H.; Hübner, H.; Vierling, W.; Brandt, W.; Reiter, M. Spiganthine, the cardioactive principle of Spigelia anthelmia. *J. Nat. Prod.* **1995**, *58* (7), 1092−1096. (b) Hübner, H.; Vierling, W.; Brandt, W.; Reiter, M.; Achenbach, H. Minor constituents of Spigelia anthelmia and their cardiac activities. *Phytochemistry* **2001**, *57* (2), 285−296.

(29) (a) Beĺanger, A.; Berney, D. J. F.; Borschberg, H. J.; Brousseau, R.; Doutheau, A.; Durand, R.; Katayama, H.; Lapalme, R.; Leturc, D. M.; Liao, C. C.; MacLachlan, F. N.; Maffrand, J. P.; Marazza, F.; Martino, R.; Moreau, C.; Saint-Laurent, L.; Saintonge, R.; Soucy, P.; Ruest, L.; Deslongchamps, P. Total Synthesis of Ryanodol. *Can. J. Chem.* **1979**, *57* (24), 3348−3354. (b) Deslongchamps, P.; Beĺanger, A.; Berney, D. J. F.; Borschberg, H. J.; Brousseau, R.; Doutheau, A.; Durand, R.; Katayama, H.; Lapalme, R.; Leturc, D. M.; Liao, C. C.; Maclachlan, F. N.; Maffrand, J. P.; Marazza, F.; Martino, R.; Moreau, C.; Ruest, L.; Saint-Laurent, L.; Saintonge, R.; Soucy, P. The Total Synthesis of (+)-Ryanodol. 1. General Strategy and Search for a Convenient Diene for the Construction of a Key Tricyclic Intermediate. *Can. J. Chem.* **1990**, *68* (1), 115−126. (c) Deslongchamps, P.; Beĺanger, A.; Berney, D. J. F.; Borschberg, H. J.; Brousseau, R.; Doutheau, A.; Durand, R.; Katayama, H.; Lapalme, R.; Leturc, D. M.; Liao, C. C.; Maclachlan, F. N.; Maffrand, J. P.; Marazza, F.; Martino, R.; Moreau, C.; Ruest, L.; Saint-Laurent, L.; Saintonge, R.; Soucy, P. The Total Synthesis of (+)-Ryanodol. 2. Model Studies for Ring B and Ring C of (+)-Anhydroryanodol. Preparation of a Key Pentacyclic Intermediate. *Can. J. Chem.* **1990**, *68* (1), 127−152. (d) Deslongchamps, P.; Beĺanger, A.; Berney, D. J. F.; Borschberg, H. J.; Brousseau, R.; Doutheau, A.; Durand, R.; Katayama, H.; Lapalme, R.; Leturc, D. M.; Liao, C. C.; Maclachlan, F. N.; Maffrand, J. P.; Marazza, F.; Martino, R.; Moreau, C.; Ruest, L.; Saint-Laurent, L.; Saintonge, R.; Soucy, P. The Total Synthesis of (+)-Ryanodol. 3. Preparation of (+)-Anhydroryanodol from a Key Pentacyclic Intermediate. *Can. J. Chem.* **1990**, *68*

(1), 153−185. (e) Deslongchamps, P.; Beĺanger, A.; Berney, D. J. F.; Borschberg, H. J.; Brousseau, R.; Doutheau, A.; Durand, R.; Katayama, H.; Lapalme, R.; Leturc, D. M.; Liao, C. C.; Maclachlan, F. N.; Maffrand, J. P.; Marazza, F.; Martino, R.; Moreau, C.; Ruest, L.; Saint-Laurent, L.; Saintonge, R.; Soucy, P. The Total Synthesis of (+)-Ryanodol. 4. Preparation of (+)-Ryanodol from (+)-Anhydroryanodol. *Can. J. Chem.* **1990**, *68* (1), 186−192.

(30) (a) Nagatomo, M.; Koshimizu, M.; Masuda, K.; Tabuchi, T.; Urabe, D.; Inoue, M. Total Synthesis of Ryanodol. *J. Am. Chem. Soc.* **2014**, *136* (16), 5916−5919. (b) Nagatomo, M.; Hagiwara, K.; Masuda, K.; Koshimizu, M.; Kawamata, T.; Matsui, Y.; Urabe, D.; Inoue, M. Symmetry-Driven Strategy for the Assembly of the Core Tetracycle of (+)-Ryanodine: Synthetic Utility of a Cobalt-Catalyzed Olefin Oxidation and α-Alkoxy Bridgehead Radical Reaction. *Chem. Eur. J.* **2016**, *22* (1), 222−229. (c) Masuda, K.; Koshimizu, M.; Nagatomo, M.; Inoue, M. Asymmetric Total Synthesis of (+)-Ryanodol and (+)-Ryanodine. *Chem. Eur. J.* **2016**, *22* (1), 230−236. (d) Koshimizu, M.; Nagatomo, M.; Inoue, M. Unified Total Synthesis of 3-epi-Ryanodol, Cinnzeylanol, Cinncassiols A and B, and Structural Revision of Natural Ryanodol and Cinnacasol. *Angew. Chem. Int. Ed.* **2016**, *55* (7), 2493–2497. (e) Nagatomo, M.; Hagiwara, K.; Masuda, K.; Koshimizu, M.; Kawamata, T.; Matsui, Y.; Urabe, D.; Inoue, M. Symmetry-Driven Strategy for the Assembly of the Core Tetracycle of (+)-Ryanodine: Synthetic Utility of a Cobalt-Catalyzed Olefin Oxidation and α-Alkoxy Bridgehead Radical Reaction. *Chem. Eur. J.* **2016**, *22* (1), 222–229. (f) Masuda, K.; Koshimizu, M.; Nagatomo, M.; Inoue, M.

Asymmetric Total Synthesis of (+)-Ryanodol and (+)-Ryanodine. *Chem. Eur. J.* **2016**, *22* (1),230–236.

(31) (a) Waterhouse, A. L.; Pessah, I. N.; Francini, A. O.; Casida, J. E.; Structural aspects of ryanodine action and selectivity. *J. Med. Chem.* **1987**, *30* (4), 710–716. (b) Welch, W.; Ahmad, S.; Airey, J.A.; Gerzon, K.; Humerickhouse, R. A.; Besch, H. R. J.; Ruest, L.; Deslongchamps, P.; Sutko, J. L. Structural determinants of high-affinity binding of ryanoids to the vertebrate skeletal muscle ryanodine receptor: a comparative molecular field analysis. *Biochemistry* **1994**, *33* (20), 6074–6085.

(32) Chuang, K. V.; Xu, C.; Reisman, S. E. A 15-Step Synthesis of (+)-Ryanodol. *Science* **2016**, *353* (6302), 912–915.

(33) Xu, C.; Han, A.; Virgil, S. C.; Reisman, S. E. Chemical Synthesis of (+)-Ryanodine and (+)-20-Deoxyspiganthine. *ACS Cent. Sci.* **2017**, *3* (4), 278–282.

(34) Xu, C.; Han, A.; Reisman, S. E. An Oxidative Dearomatization Approach To Prepare the Pentacyclic Core of Ryanodol. *Org. Lett.* **2018**, *20* (13), 3793–3796.

(35) Khand, I. U.; Knox, G. R.; Pauson, P. L.; Watts, W. E.; Foreman, M. I. Organocobalt complexes. Part II. Reaction of acetylenehexacarbonyldicobalt complexes, $(R_1C_2R_2)Co_2(CO)_6$, with norbornene and its derivatives. *J. Chem. Soc. Perkin Trans. 1* **1973**, 977−981.

(36) Chuang, K. V. A Total Synthesis of (+)-Ryanodol. PhD Thesis, California Institute of Technology: Pasadena, CA, 2016. DOI: 10.7907/Z95X26ZV

(37) Egi, M., Ota, Y.; Nishimura, Y.; Shimizu, K.; Azechi, K.; Akai, S. Efficient intramolecular cyclizations of phenoxyethynyl diols into multisubstituted α, β-

unsaturated lactones. *Org. Lett.* **2013**, *15* (16), 4150–4153.

(38) Koga, Y.; Kobayashi, T.; Narasaka, K. Rhodium-catalyzed intramolecular Pauson-Khand reaction. *Chem. Lett.* **1998**, *27* (3), 249–250.

(39) Riley, H. L.; Morley, J. F.; Friend, N. A. C.; 255. Selenium dioxide, a new oxidising agent. Part I. Its reaction with aldehydes and ketones. *J. Chem. Soc. Res.* **1932**, 1875–1883.

(40) Masuda, K.; Nagatomo, M.; Inoue, M. Chemical Conversion of Ryanodol to Ryanodine. *Chem. Pharm. Bull.* **2016**, *64*, 874−879.

(41) González-Coloma, A.; Terrero, D.; Perales, A.; Escoubas, P.; Fraga, B. M. Insect Antifeedant Ryanodane Diterpenes from Persea Indica. *J. Agric. Food Chem.* **1996**, *44* (1), 296–300.

(42) Ling, S.-Q.; Xu, Y.-N.; Gu, Y.-P.; Liu, S.-Y.; Tang, W.-W. Toxicity and Biochemical Effects of Itol A on the Brown Planthopper, Nilaparvata Lugens (Stål) (Hemiptera: Delphacidae). *Pestic. Biochem. Physiol.* **2018**, *152*, 90–97.

(43) (a) Nohara, T.; Kashiwada, Y.; Tomimatsu, T.; Kido, M.; Tokubuchi, N.; Nishioka, I. Cinncassiol D1 and Its Glucoside, Novel Pentacyclic Diterpenes from Cinnamomi Cortex. *Tetrahedron Lett.* **1980**, *21* (27), 2647–2648. (b) Chai, X.-Y.; Bai, C.-C.; Shi, H.-M.; Xu, Z.-R.; Ren, H.-Y.; Li, F.-F.; Lu, Y.-N.; Song, Y.-L.; Tu, P.-F. Six Insecticidal Isoryanodane Diterpenoids from the Bark and Twigs of Itoa Orientalis. *Tetrahedron* **2008**, *64* (24), 5743–5747. (c) Zeng, J.; Xue, Y.; Shu, P.; Qian, H.; Sa, R.; Xiang, M.; Li, X.-N.; Luo, Z.; Yao, G.; Zhang, Y. Diterpenoids with Immunosuppressive Activities from Cinnamomum Cassia. *J. Nat. Prod.* **2014**,

77 (8), 1948–1954.

(44) Koshimizu, M.; Nagatomo, M.; Inoue, M. Construction of a Pentacyclic Ring System of Isoryanodane Diterpenoids by SmI_2-Mediated Transannular Cyclization. *Tetrahedron* **2018**, *74* (26), 3384–3390.

(45) Han, A.; Tao, Y.; Reisman, S. E. A 16-Step Synthesis of the Isoryanodane Diterpene (+)-Perseanol. *Nature* **2019**, *573* (7775), 563–567.

(46) Shen, Y.; Li, L.; Pan, Z.; Wang, Y.; Li, J.; Wang, K.; Wang, X.; Zhang, Y.; Hu, T.; Zhang, Y. Protecting-group-free total synthesis of (−)-jiadifenolide: development of a [4 + 1] annulation toward multisubstituted tetrahydrofurans. *Org. Lett*. 2015, *17* (21), 5480–5483.

(47) (a) Denmark, S. E.; Beutner, G. L. Lewis Base Catalysis in Organic Synthesis. *Angew. Chem. Int. Ed.* **2008**, *47* (9), 1560–1638. (b) Corey, E. J.; Link, J. O. A new chiral catalyst for the enantioselective synthesis of secondary alcohols and deuterated primary alcohols by carbonyl reduction. *Tetrahedron Lett*. **1989**, *30* (46), 6275–6278.

(48) Ueda, T.; Konishi, H.; Manabe, K. Palladium-catalyzed fluorocarbonylation using *N*-formylsaccharin as CO source: general access to carboxylic acid derivatives. *Org. Lett*. **2013**, *15* (20), 5370–5373.